Tunable photonic differentiator and integrator with a silicon microring resonator*

Jianji Dong, Ting Yang, Aoling Zheng, Xinliang Zhang
Wuhan National Lab for Optoelectronics,
Huazhong University of Science and Technology
Wuhan, China
jjdong@mail.hust.edu.cn

Linjie Zhou, Liangjun Lu, Jianping Chen
State Key Laboratory of Advanced Optical Communication Systems and Networks, Department of Electronic Engineering, Shanghai Jiao Tong University
Shanghai, China

Abstract—In this talk, we review some progresses on tunable fractional photonic differentiator and first-order linear ordinary differential equation solver with an electronically tuned microring resonator.

Keywords—photonic computing; silicon photonics; ordinary differential equation solver

I. INTRODUCTION

Photonic integrated circuits for photonic computing open up the possibility for the realization of ultrahigh-speed and ultra wide-band signal processing with compact size and low power consumption. As we know, two important parts of photonic computing are differential and integral. Photonic differentiator (DIFF) has wide applications in numerous fields such as pulse characterization, ultra-fast signal generation, and ultra-high-speed coding. And one of the most important application of integral is to solve the differential equations, which can be used in many field of science and engineering, such as temperature diffusion processes, physical problems of motion subject to acceleration inputs and frictional forces, and the response of different resistor-capacitor circuits, etc.

DIFFs can be achieved by nonlinear effects of semiconductor optical amplifiers (SOAs) [1, 2], incoherent photonic processors [3] and highly nonlinear fibers [4]. The typical schemes to solve the differential equation have focused on two routes toward solving first-order all-optical ordinary differential equation (ODE). The first one requires an optical feedback loop [5, 6], while the second one is based on a Fabry-Perot (FP) resonance cavity with properly designed temporal impulse response [7]. Nevertheless, the configurations of these schemes are bulky and complex, involving either redundant loop [5, 6] or additional optical pump [6, 7].

In this paper, we review several schemes of ultrafast photonic differentiator and integrator based on silicon integrated microring resonators. We demonstrate a fractional-order DIFF and linear ODE solver with constant-coefficient tunable based on a single microring.

II. FRACTIONAL DIFFERENTIATOR

An *N*th-order temporal differentiator provides the *N*th-order derivation of the complex envelope of an input optical signal. Therefore, the output differentiated signal in frequency domain can be written by [8]

$$E_{out}(\omega)=\left[j(\omega-\omega_0)\right]^N E_{in}(\omega) \tag{1}$$

where N is not necessarily an integer generalized to fractional-order differentiation, ω and ω_0 are the optical frequency and the carrier frequency, E_{in} and E_{out} are the input and output optical fields, respectively. An optical filter with a frequency response given by Eq. (1) can be implemented using a silicon-on-insulator (SOI) microring resonator (MRR). Mathematically, the frequency response of an MRR can be expressed as

$$T=\frac{E_{out}}{E_{in}}=\frac{r-\alpha e^{j\varphi}}{1-\alpha r e^{j\varphi}} \tag{2}$$

where $\varphi=2\pi n_{eff}L/\lambda$ is the total round trip phase accumulation, L is the ring cavity length, α is the ring propagation loss factor, n_{eff} is the wavelength effective index, λ is the wavelength in vacuum, and r is the transmission coefficient.

In the under-coupling regime, a phase shift of less than π can be achieved. The loss factor α decreases when voltages is applied on the MRR. The effect of changing α on the resonance and the phase change is shown in Fig. 1. The transmission coefficient is constant, and the loss factor is changed. As can be seen in Fig. 1(b), by decreasing α from 0.960 to 0.952, the phase shift is changed from π to 0.6π.

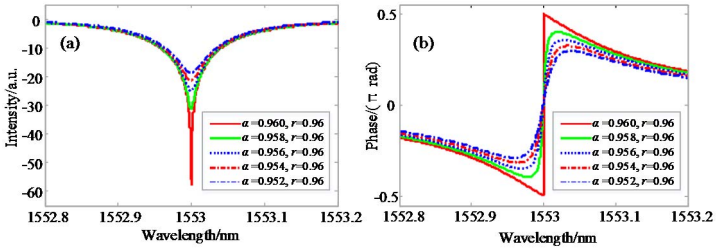

Fig. 1. The magnitude (a) and phase response (b) of the MRR operating at 1553 nm for different value of α

We then employ on-chip MRR structure to implement fractional-order differentiation. We design and fabricate the

978-1-4799-4146-9/14/$31.00 ©2014 IEEE

MRR on an SOI wafer. The thickness of the top silicon and the buried oxide layer of the SOI wafer are 220 nm and 2 μm, respectively. Deep ultra-violet (DUV) photolithography using a 248 nm stepper was employed to define the waveguide patterns, followed by anisotropic dry etch of silicon. Boron and phosphorus ion implantations were performed to form the highly *p*-type and *n*-type doped regions. Also the slab layer was etched outside the p-i-n junctions to confine the current flow around the ring waveguide. Finally, contact holes were etched and aluminum was deposited to form the metal connection. The whole fabrication process is done using CMOS compatible processes. We use vertical grating coupling method to couple the fiber and the silicon MRR. Fig. 2 shows the micrographs of (a) the fabricated MRR, (b) the zoom-in ring region.

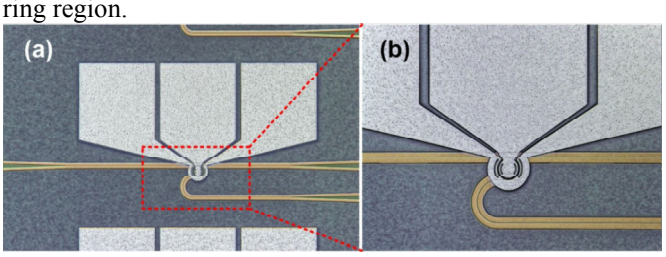

Fig. 2. (a)Microscope image of the fabricated MRR, (b) microscope image of the zoom-in ring region.

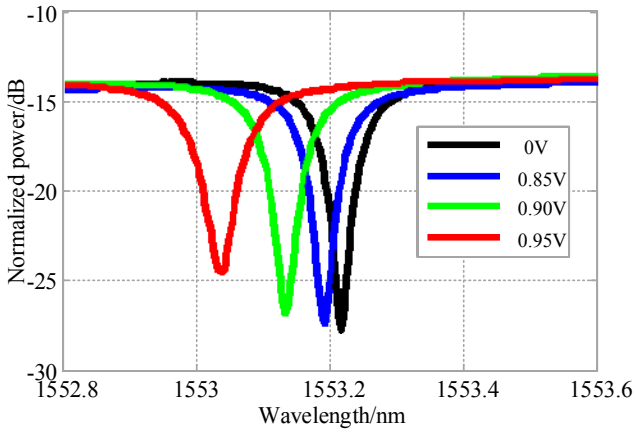

Fig. 3. Measured magnitude response of the MRR in transmission at different voltages.

Fig. 3 shows the measured magnitude response of the MRR. We apply voltages of 0.00V, 0.85V, 0.90V, and 0.95V on the MRR, respectively. The notch depth decreases with the voltage increases. Comparing the amplitude responses in Fig. 1 (a) and Fig. 3, we can see that when the applied voltage is 0V, there is the deepest frequency notch, indicating a phase shift closest approach to π at the frequency notch. As the applied voltage increases, phase shift of the MRR decreases. When the voltage is changed by 0.1V, the resonance wavelength is shifted by about 0.08nm correspondingly. Therefore the optical carrier of the signal to be differentiated should be tuned correspondingly. The total loss (including the coupling losses on both sides) of the MRR chip is about 14dB. The 3-dB bandwidth is about 10GHz. The notch depth ranges from 27dB to 24dB when applying different voltages. Due to the hardware restraint, the phase response of the MRR chip was not measured. However, we can deduce from Fig. 1 and Fig. 3 that the MRR has a varied phase shift at the resonant frequency by applying different voltages.

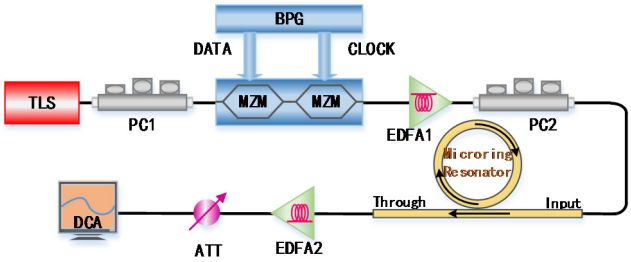

Fig. 4. Experimental setup for the fractional order differentiator with on chip MRR structure.

An experiment based on the setup shown in Fig. 4 is performed. A continuous wave (CW) is emitted by a tunable laser source (TLS) with a tuning resolution of 0.01 nm, which can be precisely aligned to the resonance wavelength of the MRR. And then the CW light is modulated by cascaded Mach-Zehnder modulators (MZMs) driven with self-coded data signal from a bit pattern generator (BPG). An erbium-doped fiber amplifier (EDFA) connected at the output of the MZMs is used to amplify the optical signal. Subsequently, the generated optical signal is coupled into the MRR using vertical grating coupling method. Polarization controllers (PCs) connected to the TLS and EDFA1 is to control and tune the polarization state of the input light to the MZMs and to the MRR, respectively. Additionally, a direct current voltage source is used to provide different voltages applied on the MRR. Then the output signal at the through port of the MRR is amplified by an EDFA and finally recorded by a digital communications analyzer (Agilent DCA86100C).

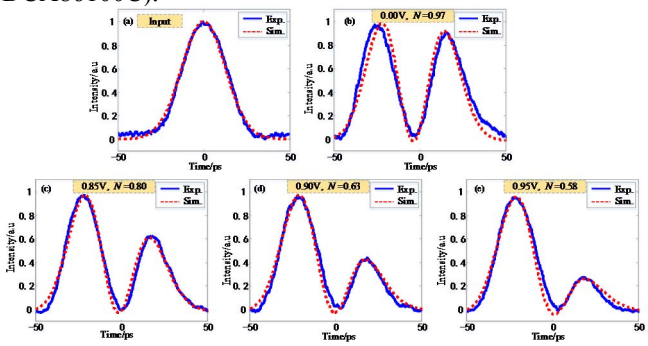

Fig. 5. (a) An input Gaussian pulse with an FWHM of 30 ps, and the differentiated pulses at the different voltages corresponding to differentiation orders of (b) N = 0.97, (c) N =0.80, (d) N =0.63, (e) N =0.58.

First, the BPG drives the two MZMs to generate a Gaussian pulse train with a pulsewidth of 30ps, as shown in Fig. 5(a). When we apply voltages of 0.00V, 0.85V, 0.90V, and 0.95V on the MRR, and fine tune the TLS wavelength to align with the resonant notch, we measure the temporal waveforms of DIFFs with fractional orders of 0.97, 0.80, 0.63, and 0.58, respectively, which are shown in Fig. 5(b)-(e), respectively. It

can be seen that the measured differentiated pulses fit well with the simulated pulses.

III. ODE SOLVER SYSTEM

Recently, we reported an ODE solver system based on electronically tuned MRR [9]. The common constant-coefficient first-order linear ODE can be expressed as:

$$\frac{dy(t)}{dt} + ky(t) = x(t) \tag{3}$$

Where $x(t)$ represents the input signal, $y(t)$ is the equation solution (output signal) and k denotes a positive constant of an arbitrary value. We know that a silicon microring functions as a loss integrator, which has a similar transfer function to Eq. (3) at the drop port. Therefore, a single add-drop microring can be utilized to solve constant-coefficient first-order linear ODE. If we change the Q value of the microring, we can build a constant-coefficient tunable ODE solver. Therefore we fabricate an electrically tuned add-drop microring as shown in Fig. 2.

We choose super-Gaussian pulse as the input signal. And when the voltage applied on the microring is 0 V, corresponding to a constant-coefficient of about 0.038/ps, the output waveform (yellow solid line) is depicted in Fig. 6(b), and the calculated waveform (red attunement line) according to the ideal ODE solver is shown for comparison. When we change the voltages to 0.9 V, 1.0 V, 1.1 V and 1.3 V, corresponding to the constant-coefficient of 0.046/ps, 0.054/ps, 0.063/ps and 0.082/ps respectively, the measured output waveforms are depicted in Figs. 6(c), (d), (e) and (f). The fitted dash lines in Fig. 5 represent the smooth processes of measured waveforms.

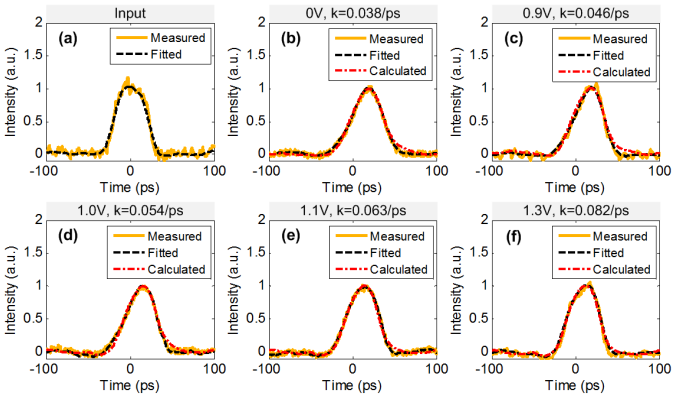

Fig. 6. Experimental results for super-Gaussian input. (a) is the input waveform; yellow solid line: measured pulse, black dash line: fitted pulse. (b), (c), (d), (e) and (f) are the outputs with different voltages applied on the MRR; yellow solid line: measured waveforms, black dash line: fitted waveforms and red attunement line: calculated ideal outputs.

IV. CONCLUSIONS

Several schemes of ultrafast photonic differentiator and integrator was proposed and experimentally demonstrated in this paper. We demonstrated tunable fractional-order DIFF and first-order linear ODE with different values of constant-coefficient employing on-chip silicon microring resonator. Our schemes show the advantages of compact footprint, flexible and versatile.

ACKNOWLEDGMENT

This work was partially supported by the National Basic Research Program of China (Grant No. 2011CB301704), the Program for New Century Excellent Talents in Ministry of Education of China (Grant No. NCET-11-0168), a Foundation for the Author of National Excellent Doctoral Dissertation of China (Grant No. 201139), the National Natural Science Foundation of China (Grant No. 60901006, and Grant No. 11174096), and the Fundamental Research Funds for the Central Universities, HUST: 2014YQ015.

REFERENCES

[1]. Xu J., X. L. Zhang and J. J. Dong, "High speed all-optical differentiator based on cascading semiconductor optical amplifier and optical filter," Opt. Lett. Vol. 32, No. 13, pp.1872-1874, 2007.

[2]. Xu J., X. L. Zhang and J. J. Dong, and D. Huang, "All-optical differentiator based on cross-gain modulation in semiconductor optical amplifier," Opt. Lett. Vol. 32, No. 20, pp.3029-3031, 2007.

[3]. Park Yongwoo, M. H. Asghari and R. Helsten, "Implementation of Broadband Microwave Arbitrary-Order Time Differential Operators Using a Reconfigurable Incoherent Photonic Processor," Photonics Journal, IEEE Vol. 2, No. 6, pp.1040-1050, 2010.

[4]. Velanas P., A. Bogris and A. Argyris, "High-Speed All-Optical First- and Second-Order Differentiators Based on Cross-Phase Modulation in Fibers," Lightwave Technology, Vol. 26, No. 18, pp.3269-3276, 2008.

[5]. Lu L. Y., J. Y. Wu and T. Wang, "Compact all-optical differential-equation solver based on silicon microring resonator," Frontiers of Optoelectronics Vol.5, No. 1, pp.99-106, 2012.

[6]. Tan S. S., Z. Wu and L. Lei, "All-optical computation system for solving differential equations based on optical intensity differentiator." Optics express Vol.21, No. 6, pp.7008-7013, 2013.

[7]. Slavík, R. Yongwoo Park and N. Ayotte. "Photonic temporal integrator for all-optical computing." Opt. Express Vol. 16, No. 22, pp.18202-18214, 2008.

[8]. J. Dong , A. Zheng, D. Gao, L. Lei, D. Huang, and X. Zhang, "Compact, flexible and versatile photonic differentiator using silicon Mach-Zehnder interferometers," Opt. Express Vol. 21, No. 6, pp.7014–7024, 2013.

[9]. T. Yang, J. Dong , L. Lu, L. Zhou, A. Zheng, X. Zhang, and J. Chen, "All-optical differential equation solver with constant-coefficient tunable based on a single microring resonator," Sci. Rep. 2014.